

Modifying optical properties of three-level V-type atomic medium by varying external magnetic field

Nguyen Huy Bang  and Le Van Doai 

Vinh University, 182 Le Duan Street, Vinh City, Vietnam

E-mail: doailv@vinhuni.edu.vn

Received 14 June 2020, revised 19 August 2020

Accepted for publication 25 August 2020

Published 7 September 2020



CrossMark

Abstract

Optical properties including absorption, dispersion, group index, Kerr nonlinearity, and optical bistability of a three-level V-type atomic medium have modified by varying an external magnetic field. By changing the magnitude or the sign of the external magnetic field, the transparency window with normal dispersion transfers to the enhanced absorption with anomalous dispersion at the line center, and hence the light propagation switches between subluminal and superluminal modes. The magnitude and the sign of the Kerr nonlinearity are controlled with the strength and the sign of the magnetic field. As a consequence, the behaviors of optical bistability are also made to appear or disappear when switching on/off the magnetic field. Moreover, the threshold intensity and width of optical bistability are also changed by the magnetic field and the coupling field. The results can be used to control the working characteristics of applied devices and study the related effects.

Keywords: electromagnetically induced transparency, group velocity, Kerr nonlinearity, optical bistability

(Some figures may appear in colour only in the online journal)

1. Introduction

Recently, modification of optical properties of an atomic medium by external fields has received considerable attention from research groups due to it can change the working characteristics of applied devices. The linear and nonlinear optical properties of the medium can be modified by quantum coherence and interference via electromagnetically induced transparency (EIT) effect [1–3]. The EIT can arise from the destructive quantum interference of the transition amplitudes which can significantly reduce resonant absorption of the probe beam propagating inside an opaque atomic medium [4]. Simplest exciting schemes of the EIT are three-level atomic systems consisting of Λ -type [5], V-type [6], and ladder-type [7] configurations. The EIT materials have interesting applications in the fields of quantum and nonlinear optics including lasing without population inversion [8], slow and fast light [9–12], enhancement of Kerr nonlinearity [13–23], controlling optical bistability [24–27], pulse propagation

[28–30], all-optical switching [31, 32], and so on. The studies demonstrated that the linear and nonlinear optical properties of materials are easily controlled according to the intensity, frequency, polarization, and phase of external light fields. To understand more deeply about these topics, readers can refer to review papers [4, 33].

Recently, many studies have been interested in using an external magnetic field to control absorption and dispersion [34–39], light propagation [40, 41], Kerr nonlinearity [42], and optical switching and bistability [43, 44]. In most of these studies, the external magnetic field is utilized to separate the degenerate sublevels of the ground-state via the Zeeman effect and form the three-level Λ -type scheme.

In this paper, we suggest using the magnetic field to remove the degeneracy among the excited-state sublevels and create a three-level V-type scheme. By solving the density matrix equations in a steady-state condition ($\dot{\rho} = 0$), we have derived the analytical expressions for first- and third-order susceptibilities as functions of laser parameters and external

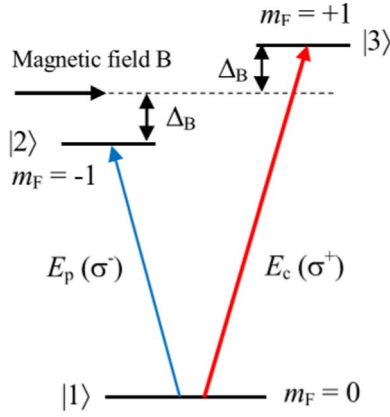


Figure 1. Degenerated three-level V-type atomic system in an external magnetic field: the state $|3\rangle$ is lifted while the state $|2\rangle$ is lowered by the same amount Δ_B corresponding to the Zeeman shift.

magnetic field. We have shown that the external magnetic field can use as a ‘knob’ to control absorption and dispersion, group index, Kerr nonlinearity, and optical bistability of the

$$H = \frac{\hbar}{2} \begin{bmatrix} 2(\Delta_p + \Delta_B) - 2(\Delta_c - \Delta_B) & \Omega_p & \Omega_c \\ \Omega_p & 2(\Delta_c - \Delta_B) & 0 \\ \Omega_c & 0 & 2(\Delta_p + \Delta_B) \end{bmatrix}. \quad (2)$$

degenerated three-level V-type EIT medium. Besides, the investigation can help us deeply understand the causal relationship between linear and nonlinear optical properties.

2. Theoretical model

The degenerated three-level V-type atomic system in an external magnetic field as shown in figure 1. The σ^- polarized probe beam (and angular frequency ω_p) E_p drives the transition $|1\rangle \leftrightarrow |2\rangle$, while the σ^+ polarized coupling beam (and angular frequency ω_c) E_c couples the transition $|1\rangle \leftrightarrow |3\rangle$. In this configuration, the magnetic field (B) is arranged parallel to the propagation direction of both probe and coupling beams and is used to separate the degenerate sublevels $|2\rangle$ and $|3\rangle$ of the excited-state via the Zeeman effect. The Zeeman shift between the sublevels $|2\rangle$ and $|3\rangle$ is determined by [42] $\hbar\Delta_B = \mu_B m_F g_F B$ with μ_B is the Bohr magneton, g_F is the Landé factor, and $m_F = \pm 1$ is the magnetic quantum number of the involved state. Spontaneous decay rates of the excited states $|2\rangle$ and $|3\rangle$ are Γ_{21} and Γ_{31} , while Γ_{32} is the relaxation rate between the levels $|2\rangle$ and $|3\rangle$ by collisions. We define the frequency detunings of the probe and coupling fields are $\Delta_p = \omega_p - \omega_{21}$ and $\Delta_c = \omega_c - \omega_{31}$, respectively. The Rabi frequencies of the probe and coupling fields are respectively determined by $\Omega_p = d_{21}E_p/\hbar$ and $\Omega_c = d_{31}E_c/\hbar$ with d_{mn} is the dipole moment for the transition $|m\rangle \leftrightarrow |n\rangle$.

The master equation of motion for the density operator describing the time evolution of the atomic system is written

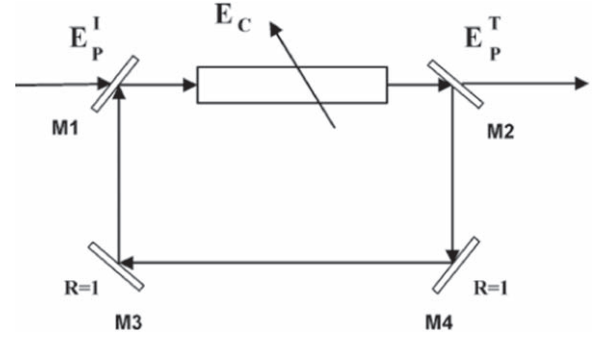


Figure 2. Unidirectional ring cavity containing an atomic medium of length L . E_p^I and E_p^T represent the incident and the transmitted probe fields, respectively.

as follows:

$$\dot{\rho} = -\frac{i}{\hbar}[H, \rho] + L\rho, \quad (1)$$

where $L\rho$ represents the relaxation processes. The total Hamiltonian has the form:

From equations (1) and (2), we obtain the density matrix equations in the presence of the external magnetic field as:

$$\begin{aligned} \dot{\rho}_{11} = & \Gamma_{31}\rho_{33} + \Gamma_{21}\rho_{22} + \frac{i}{2}\Omega_p(\rho_{21} - \rho_{12}) \\ & + \frac{i}{2}\Omega_c(\rho_{31} - \rho_{13}), \end{aligned} \quad (3)$$

$$\dot{\rho}_{22} = -(\Gamma_{21} + \Gamma_{32})\rho_{22} + \frac{i}{2}\Omega_p(\rho_{12} - \rho_{21}), \quad (4)$$

$$\dot{\rho}_{33} = -\Gamma_{31}\rho_{33} + \Gamma_{32}\rho_{22} + \frac{i}{2}\Omega_c(\rho_{13} - \rho_{31}), \quad (5)$$

$$\begin{aligned} \dot{\rho}_{21} = & [i(\Delta_p + \Delta_B) - \gamma_{21}]\rho_{21} + \frac{i}{2}\Omega_p(\rho_{11} - \rho_{22}) \\ & - \frac{i}{2}\Omega_c\rho_{23}, \end{aligned} \quad (6)$$

$$\begin{aligned} \dot{\rho}_{31} = & [i(\Delta_c - \Delta_B) - \gamma_{31}]\rho_{31} + \frac{i}{2}\Omega_c(\rho_{11} - \rho_{33}) \\ & - \frac{i}{2}\Omega_p\rho_{32}, \end{aligned} \quad (7)$$

$$\begin{aligned} \dot{\rho}_{23} = & [i(\Delta_p - \Delta_c + 2\Delta_B) - \gamma_{32}]\rho_{23} + \frac{i}{2}\Omega_p\rho_{13} \\ & - \frac{i}{2}\Omega_c\rho_{21}, \end{aligned} \quad (8)$$

$$\rho_{nm} = \rho_{mn}^*, \quad (9)$$

$$\rho_{11} + \rho_{22} + \rho_{33} = 1. \quad (10)$$

where γ_{mn} is the dephasing rate of atomic coherence ρ_{mn} which is related to the spontaneous decay rate Γ_{mn} as follows:

$$\gamma_{mn} = \frac{1}{2} \left(\sum_{k < m} \Gamma_{mk} + \sum_{l < n} \Gamma_{nl} \right). \quad (11)$$

In order to investigate the linear and nonlinear optical properties of the materials, we need to derive the expressions of the linear and nonlinear susceptibilities by finding the solution of density matrix equations up to third-order perturbation (under the steady-state condition) via an iterative technique. That is, the density matrix elements are expanded as:

$$\rho_{mn} = \rho_{mn}^{(0)} + \rho_{mn}^{(1)} + \dots + \rho_{mn}^{(n)}, \quad (12)$$

Assuming that the atom initially populates in the ground state $|1\rangle$, $\rho_{11}^{(0)} \approx 1$, while $\rho_{22}^{(0)} \approx \rho_{33}^{(0)} \approx 0$. In the weak probe field approximation, the solution of the density matrix element ρ_{21} in first-order can be found from equations (6) and (8) as follows:

$$\begin{aligned} \rho_{21}^{(1)} &= \frac{\frac{i}{2} \Omega_p (\rho_{22}^{(0)} - \rho_{11}^{(0)})}{\gamma_{21} - i(\Delta_p + \Delta_B) + \frac{(\Omega_c/2)^2}{\gamma_{32} - i(\Delta_p - \Delta_c + 2\Delta_B)}} \\ &\approx \frac{-i\Omega_p}{2D}, \end{aligned} \quad (13)$$

where

$$D = \gamma_{21} - i(\Delta_p + \Delta_B) + \frac{(\Omega_c/2)^2}{\gamma_{32} - i(\Delta_p - \Delta_c + 2\Delta_B)}. \quad (14)$$

Similarly, the expression for ρ_{21} in third-order has the form:

$$\rho_{21}^{(3)} = \frac{i\Omega_p (\rho_{22}^{(2)} - \rho_{11}^{(2)})}{2D}. \quad (15)$$

From equations (3) and (5), $\rho_{22}^{(2)} - \rho_{11}^{(2)}$ can be determined as follows:

$$\rho_{22}^{(2)} - \rho_{11}^{(2)} = \frac{i\Omega_p (\rho_{21}^{(1)} - \rho_{12}^{(1)})}{\Gamma_{21}} \equiv \frac{\Omega_p^2}{2\Gamma_{21}} \left(\frac{1}{D} + \frac{1}{D^*} \right). \quad (16)$$

Therefore, ρ_{21} in third-order is calculated as:

$$\rho_{21}^{(3)} = \frac{\Omega_p^2}{2\Gamma_{21}} \frac{i\Omega_p}{D} \left[\frac{1}{D} + \frac{1}{D^*} \right]. \quad (17)$$

Finally, the density matrix element ρ_{21} up to third-order can be obtained as:

$$\rho_{21} = \rho_{21}^{(1)} + \rho_{21}^{(3)} = \frac{-i\Omega_p}{2D} + \frac{i\Omega_p}{2D} \frac{\Omega_p^2}{\Gamma_{21}} \left(\frac{1}{D} + \frac{1}{D^*} \right), \quad (18)$$

here D^* is the complex conjugation of D .

The probe susceptibility χ is proportional to ρ_{21} through the following expression:

$$\chi = -2 \frac{Nd_{21}}{\varepsilon_0 E_p} \rho_{21} \equiv \frac{Nd_{21}}{\varepsilon_0 E_p} \left[\frac{i\Omega_p}{2D} - \frac{i\Omega_p}{2D} \frac{\Omega_p^2}{\Gamma_{21}} \left(\frac{1}{D} + \frac{1}{D^*} \right) \right]. \quad (19)$$

where N is the number density of atoms, ε_0 is the free space permittivity.

On the other hand, the probe susceptibility can also be presented in an alternative form as:

$$\chi = \chi^{(1)} + 3E_p^2 \chi^{(3)}. \quad (20)$$

From equations (19) and (20) we derive the first-order susceptibility $\chi^{(1)}$ and the third-order susceptibility $\chi^{(3)}$ as the functions of laser parameters and external magnetic field:

$$\chi^{(1)} = \frac{Nd_{21}^2}{\varepsilon_0 \hbar} \left(\frac{P}{P^2 + Q^2} + i \frac{P}{P^2 + Q^2} \right), \quad (21)$$

$$\chi^{(3)} = -\frac{Nd_{21}^4}{3\varepsilon_0 \hbar^3} \frac{1}{\Gamma_{21}} \frac{Q}{P^2 + Q^2} \left(\frac{P}{P^2 + Q^2} + i \frac{Q}{P^2 + Q^2} \right), \quad (22)$$

where the expressions P and Q are determined by

$$P = -(\Delta_p + \Delta_B) + \frac{(\Delta_p - \Delta_c + 2\Delta_B)}{\gamma_{32}^2 + (\Delta_p - \Delta_c + 2\Delta_B)^2} \left(\frac{\Omega_c}{2} \right)^2, \quad (23)$$

$$Q = \gamma_{21} + \frac{\gamma_{32}}{\gamma_{32}^2 + (\Delta_p - \Delta_c + 2\Delta_B)^2} \left(\frac{\Omega_c}{2} \right)^2, \quad (24)$$

Based on the first-order susceptibility, we determine the linear absorption α and dispersion n_0 as:

$$\alpha = \frac{Nd_{21}^2 \omega_p}{2c\varepsilon_0 \hbar} \frac{Q}{P^2 + Q^2}, \quad (25)$$

$$n_0 = 1 + \frac{\text{Re}(\chi^{(1)})}{2} = 1 + \frac{Nd_{21}^2}{2\varepsilon_0 \hbar} \frac{P}{P^2 + Q^2}. \quad (26)$$

These expressions will be used to study the control of absorption and dispersion coefficients according to the external magnetic field. As a consequence, the change in the dispersion can lead to the modification of the group velocity which is defined as follows:

$$v_g = \frac{c}{n_g}, \quad (27)$$

with c is the speed of light in vacuum, n_g is the group index that defined as

$$n_g = n_0 + \omega_p \frac{dn_0}{d\omega_p} \simeq \omega_p \frac{Nd_{21}^2}{2\varepsilon_0\hbar} \times \left[\frac{P'(P^2 + Q^2) - 2P(PP' + QQ')}{(P^2 + Q^2)^2} \right]. \quad (28)$$

where P' and Q' are respectively the derivatives of P and Q over ω_p , that given by:

$$P' = -1 + \frac{(\Omega_c/2)^2}{\gamma_{32}^2 + (\Delta_p - \Delta_c + 2\Delta_B)^2} - \frac{2(\Delta_p - \Delta_c + 2\Delta_B)^2}{[\gamma_{32}^2 + (\Delta_p - \Delta_c + 2\Delta_B)^2]^2} \left(\frac{\Omega_c}{2} \right)^2, \quad (29)$$

$$Q' = -\frac{2\gamma_{32}(\Delta_p - \Delta_c + 2\Delta_B)}{[\gamma_{32}^2 + (\Delta_p - \Delta_c + 2\Delta_B)^2]^2} \left(\frac{\Omega_c}{2} \right)^2. \quad (30)$$

On the other hand, from the third-order susceptibility we obtain the self-Kerr nonlinear coefficient n_2 as follows:

$$n_2 = \frac{3 \operatorname{Re}(\chi^{(3)})}{4\varepsilon_0 n_0^2 c} \equiv -\frac{Nd_{21}^4}{4\varepsilon_0^2 \hbar^3 c} \frac{1}{\Gamma_{21}} \times \frac{PQ}{\left(1 + \frac{Nd_{21}^2}{2\varepsilon_0 \hbar} \frac{P}{P^2 + Q^2} \right) (P^2 + Q^2)^2}. \quad (31)$$

To see the advantage of controllable Kerr nonlinearity, we apply this Kerr nonlinear medium to the optical bistability device. We put the atomic sample of length L containing N degenerated three-level V-type atomic system into a unidirectional ring cavity (figure 2). We denote R and T are the reflection and transmission coefficient of mirrors M1 and M2 with $R + T = 1$. Assuming that mirrors M3 and M4 have 100% reflectivity. The probe beam E_p circulates in the ring cavity, while the coupling beam E_c do not.

The total electromagnetic field is represented by

$$E = E_p e^{-i\omega_p t} + E_c e^{-i\omega_c t} + c.c., \quad (32)$$

The dynamic equation of the probe field under the slowly varying envelop approximation is:

$$\frac{\partial E_p}{\partial t} + c \frac{\partial E_p}{\partial z} = i \frac{\omega_p}{2\varepsilon_0} P(\omega_p), \quad (33)$$

with $P(\omega_p)$ is polarization induced by the probe field:

$$P(\omega_p) = Nd_{21} \rho_{21}. \quad (34)$$

From equations (33) and (34), the probe field amplitude in the steady state can be written as:

$$\frac{\partial E_p}{\partial z} = i \frac{N\omega_p d_{21}}{2c\varepsilon_0} \rho_{21}. \quad (35)$$

For a perfectly tuned cavity, in the steady state, the boundary conditions for the incident field (E_p^I) and the transmitted field (E_p^T) are

$$E_p(L) = E_p^T / \sqrt{T}, \quad (36)$$

$$E_p(0) = \sqrt{T} E_p^I + R E_p(L). \quad (37)$$

where R is the feedback mechanism from the mirror M2, which is an essential element to optical bistability. In the mean-field limit and associating with the boundary condition equations, we derive the input-output amplitude relationship for the probe beam:

$$Y = X - iC\rho_{21}, \quad (38)$$

where $Y = d_{21} E_p^I / (\hbar\sqrt{T})$, $X = d_{21} E_p^T / (\hbar\sqrt{T})$ are normalized input and output fields, respectively; $C = \frac{N\omega_p L d_{21}^2}{2c\varepsilon_0 \hbar T}$ is cooperation parameter. Thus, the transmitted probe field depends on the incident probe field and the coherence term ρ_{21} via equation (38). Therefore, the bistable behaviors can be identified by atomic variables through ρ_{21} which can find from equations (3)–(10).

3. Results and discussion

Now, we apply the theoretical model to ^{87}Rb atoms with the levels $|1\rangle$, $|2\rangle$ and $|3\rangle$ corresponding to the states $5S_{1/2}$ ($F = 1, m_F = 0$), $5P_{3/2}$ ($F = 2, m_F = -1$), and $5P_{3/2}$ ($F = 2, m_F = +1$). The parameters are taken to be [43]: $N = 4.5 \times 10^{17}$ atoms/m³, $\Gamma_{21} = \Gamma_{31} = 5.7$ MHz and $\gamma_{21} = \gamma_{31} = \gamma_{23} = 3$ MHz, $d_{21} = 1.6 \times 10^{-29}$ C.m. The Landé factor $g_F = -1/2$, and the Bohr magneton $\mu_B = 9.274 01 \times 10^{-24}$ JT⁻¹. In the following investigations, all the parameters related to frequency are scaled with $\gamma = 2\pi \times 1$ MHz. In this way, the Zeeman shift Δ_B can also be expressed in γ , and hence the magnetic field strength B is scaled by $\gamma_c = \hbar\mu_B^{-1} m_F^{-1} g_F^{-1} \gamma$. For instance, if the Zeeman shift $\Delta_B = 14\gamma$ then the magnetic field strength $B = \Delta_B \hbar / (\mu_B m_F g_F) = 14\gamma_c$.

3.1. Modifying linear optical properties

First, we consider the absorption and dispersion properties of the medium for the probe beam in the absence $B = 0$ (solid line) and the presence $B = \pm 14\gamma_c$ (dashed line) of the external magnetic field, as presented in figures 3 and 4, respectively. Where, the coupling parameters are $\Omega_c = 40\gamma$ and $\Delta_c = 0$. From figure 3, we can see that by choosing the external magnetic field $B = -14\gamma_c$ or and $B = 14\gamma_c$, electromagnetically induced transparency (EIT) at the resonant frequency is converted to electromagnetically induced absorption (EIA). At the same time, strong absorption peaks at the positions of $\Delta_p = 20\gamma$ or $\Delta_p = -20\gamma$ is transformed into the transparency windows.

As a consequence, the normal dispersions in transparency windows are also changed to anomalous dispersions in strong absorption regions and vice versa, via turn-on/off of the magnetic field as depicted in figure 4. These lead to the group velocity is also switched from subluminal to superluminal and

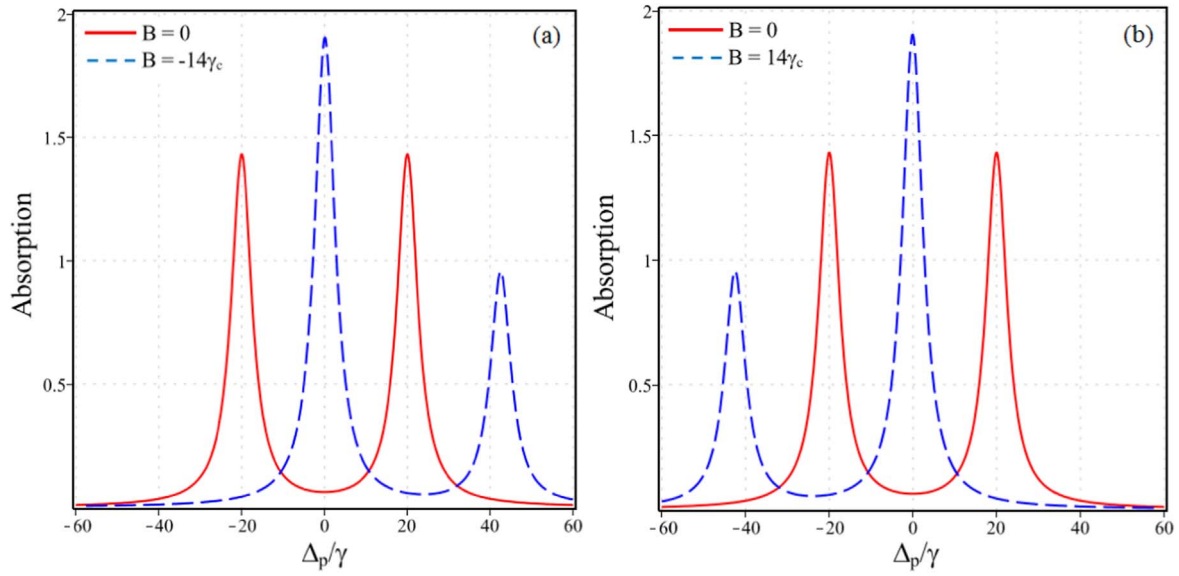


Figure 3. Variations of absorption versus probe detuning in the absence $B = 0$ (solid line) and the presence (dashed line) of the external magnetic field $B = -14\gamma_c$ (a) and $B = 14\gamma_c$ (b). The coupling parameters are $\Omega_c = 40\gamma$ and $\Delta_c = 0$.

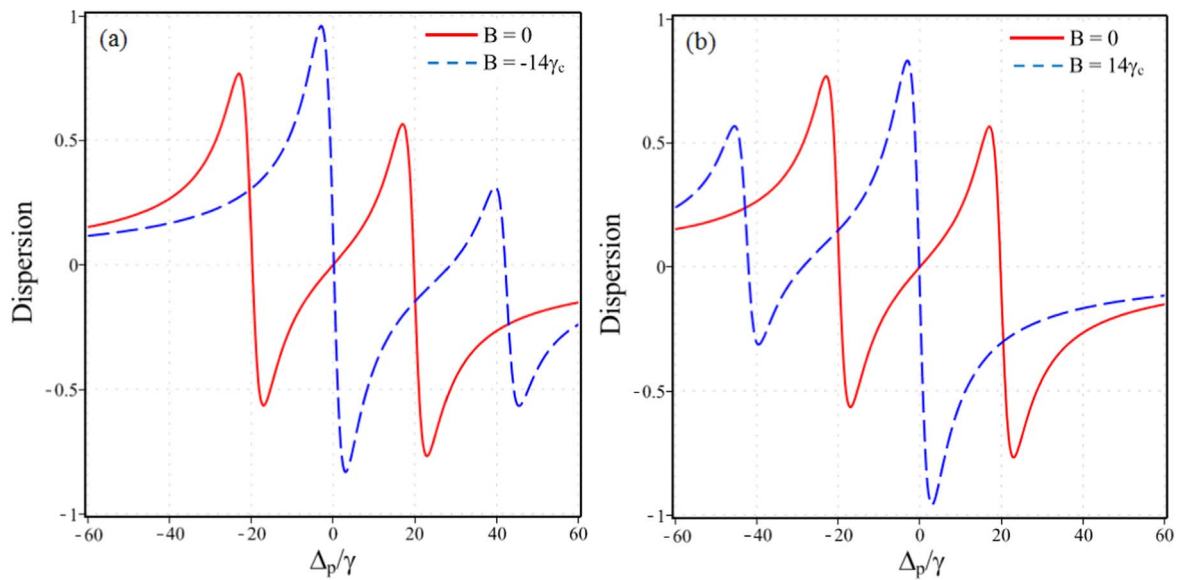


Figure 4. Variations of dispersion versus probe detuning in the absence $B = 0$ (solid line) and the presence (dashed line) of the external magnetic field $B = -14\gamma_c$ (a) and $B = 14\gamma_c$ (b). The parameters of the coupling field are fixed at $\Omega_c = 40\gamma$ and $\Delta_c = 0$.

vice versa, as described in figure 5. Specifically, the subluminal light regime in the resonant region when $B = 0$ is converted to a superluminal light regime when $B = -14\gamma_c$ or $B = 14\gamma_c$. Otherwise, the subluminal regime at the positions of $\Delta_p = 20\gamma$ or $\Delta_p = -20\gamma$ when $B = 0$ are transformed to the superluminal regime when $B = -14\gamma_c$ or $B = 14\gamma_c$.

In figure 6, we present the variation of group index versus the external magnetic field when $\Delta_p = \Delta_c = 0$ and $\Omega_c = 40\gamma$, which corresponds to the subluminal regime when $B = 0$. The variation in figure 6 shows that both the magnitude and the sign of the group index is changed with respect

to the magnetic field. That is, for the given values of parameters Δ_c , Δ_p and Ω_c we can choose an optimized magnetic field to attain the maximum value of the group index.

3.2. Modifying nonlinear optical properties

Next, we investigate the influence of the magnetic field on the amplitude and the sign of Kerr-nonlinear coefficient as depicted in figure 7. Here, we have plotted the Kerr nonlinear coefficient versus the probe detuning when $B = 0$ and $B = \pm 13\gamma_c$. Figure 7 shows that the zero value of Kerr nonlinear coefficient at

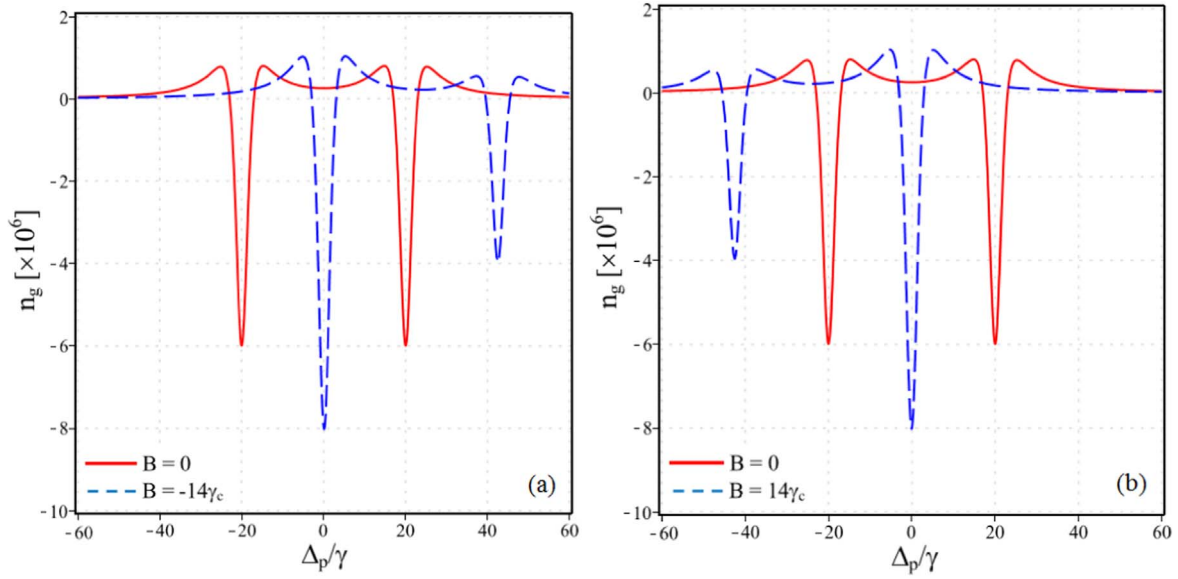


Figure 5. Variations of the group index versus probe detuning in the absence $B = 0$ (solid line) and the presence (dashed line) of the external magnetic field $B = -14\gamma_c$ (a) and $B = 14\gamma_c$ (b). The parameters of the coupling field are fixed at $\Omega_c = 40\gamma$ and $\Delta_c = 0$.

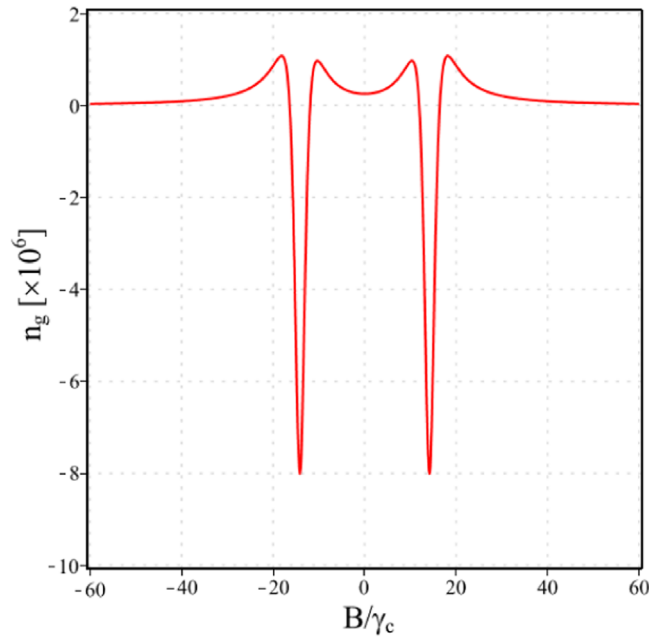


Figure 6. Variation of the group index versus the external magnetic field when $\Delta_p = 0$, $\Delta_c = 0$ and $\Omega_c = 40\gamma$.

two-photon resonance of probe and coupling lights ($\Delta_p = \Delta_c = 0$) and $\Omega_c = 40\gamma$ in the case of $B = 0$ is transformed to the positive peak when $B = -13\gamma_c$ or the negative peak when $B = 13\gamma_c$. At the same time, frequency regions with positive nonlinearity can be switched into those with negative nonlinearity and vice versa. In addition, from figure 7 we can see that the negative peak of Kerr nonlinear coefficient at $\Delta_p = 19\gamma$ or the positive peak at $\Delta_p = -19\gamma$ in the case of $B = 0$ is transformed to the zero points when $B = -13\gamma_c$ or $B = 13\gamma_c$, respectively. Similar to linear dispersion, moreover, the nonlinear dispersion is

also changed from normal to anomalous when turn-on/off of the magnetic field.

In order to see the change of Kerr nonlinear coefficient versus the magnetic field, we fix the parameters of the probe and coupling fields at $\Delta_p = \Delta_c = 0$ and $\Omega_c = 40\gamma$ (that corresponds to the zero point of Kerr nonlinear coefficient when $B = 0$), and plot nonlinear coefficient with respect to the magnetic field as represented in figure 8. It is also shown that both the magnitude and the sign of the Kerr nonlinearity are controlled with the external magnetic field. This means that we can choose the

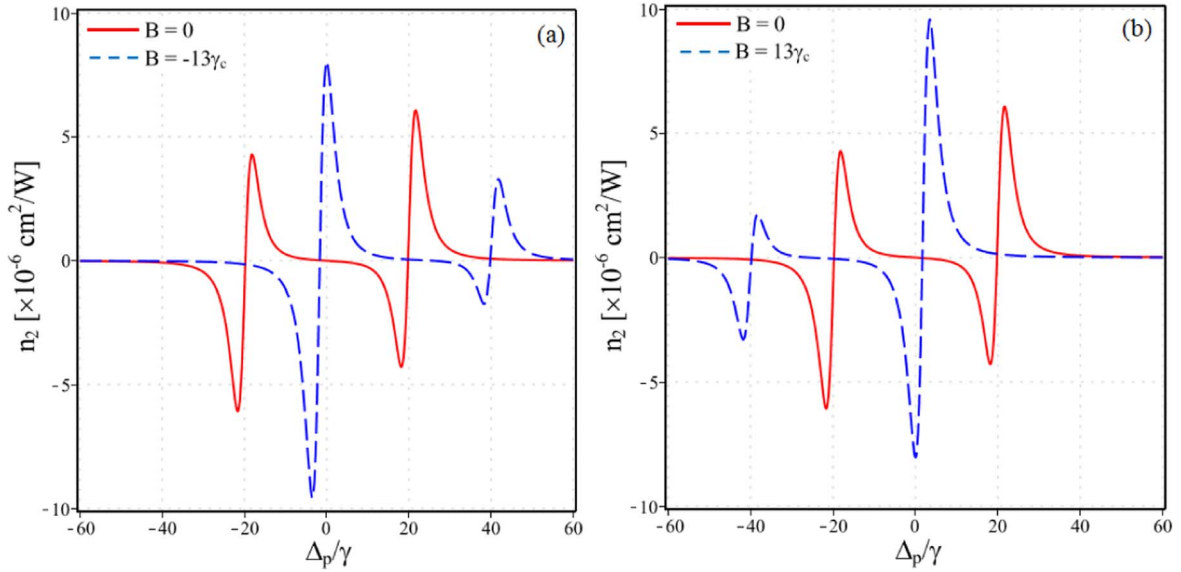


Figure 7. Variations of Kerr nonlinear coefficient versus probe detuning in the absence $B = 0$ (solid line) and the presence (dashed line) of the external magnetic field $B = -13\gamma_c$ (a) and $B = 13\gamma_c$ (b). The coupling parameters are $\Omega_c = 40\gamma$ and $\Delta_c = 0$.

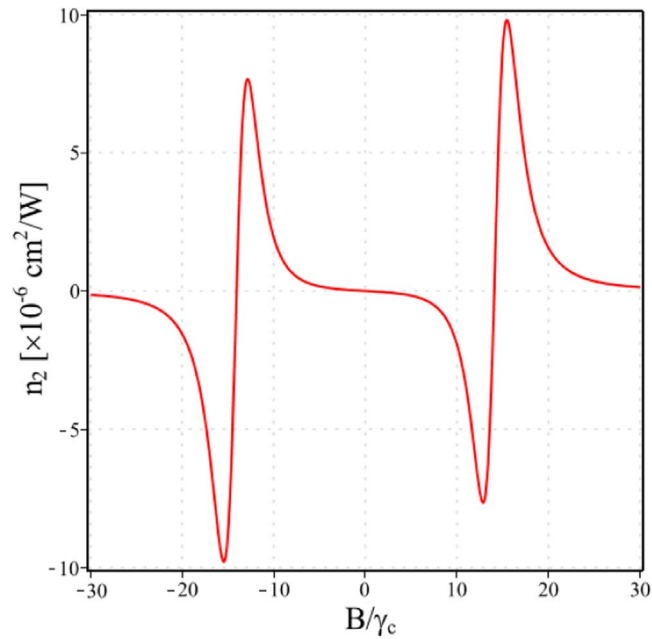


Figure 8. Variation of Kerr nonlinear coefficient versus the external magnetic field when $\Delta_p = 0$, $\Delta_c = 0$ and $\Omega_c = 40\gamma$.

appropriate magnetic field to achieve the optimum value of the Kerr nonlinearity. This is important to control the characteristics of optical bistability (OB) that will examine below.

In figure 9 we consider the variation of the negative peak of nonlinear coefficient at $\Delta_p = \Delta_c = 0$, $\Omega_c = 40\gamma$ and $B = 13\gamma_c$ (see the dashed line of figure 7(a)) with respect to the Rabi frequency (a) and the frequency detuning (b) of the coupling field. It shows that the magnitude and the sign of the Kerr nonlinearity can also be changed by tuning the intensity or frequency of the coupling beam. That is, with given

parameters of the probe field and the magnetic field we can adjust the intensity or the frequency of the coupling field to obtain the negative, positive, or zero values of the Kerr nonlinear coefficient.

Finally, we apply such a controllable nonlinear coefficient to the OB device and control the characteristics of the OB as in figures 10 and 11. For figure 10, we plotted the input-output intensity of the OB when $\Delta_p = 0$ (a) and $\Delta_p = 19\gamma$ (b) in the absence ($B = 0$) and the presence ($B = -13\gamma_c$) of the magnetic field. Where, the coupling

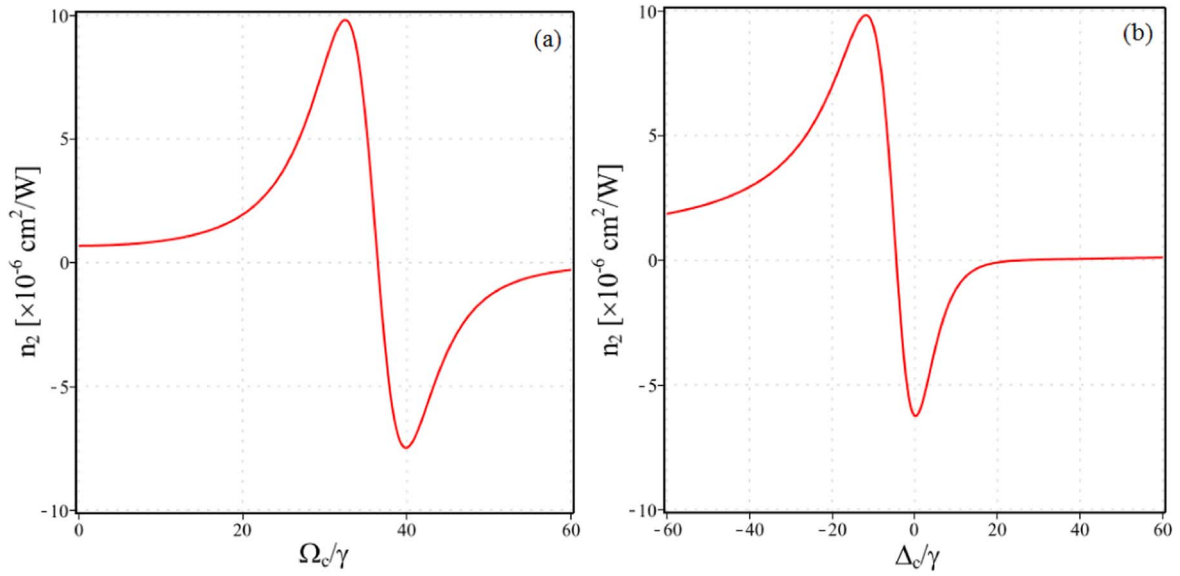


Figure 9. Variations of Kerr nonlinear coefficient versus the intensity when $\Delta_c = 0$ (a) and the frequency detuning when $\Omega_c = 40\gamma$ (b) of the coupling field. Other parameters are $\Delta_p = 0$ and $B = 13\gamma_c$.

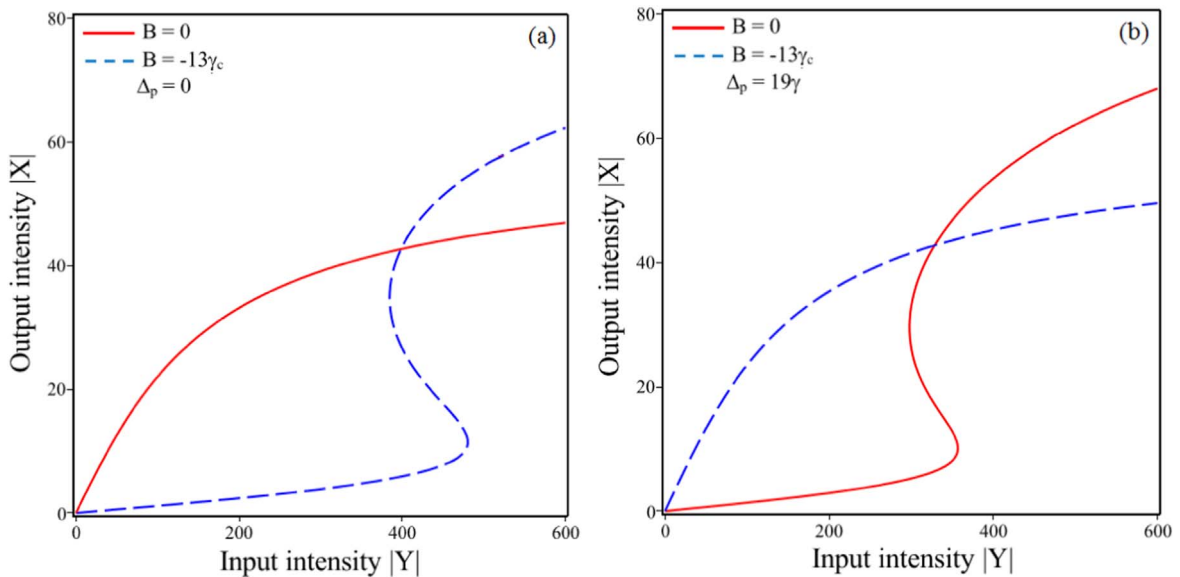


Figure 10. The input–output intensity curves in the absence $B = 0$ (solid line) and the presence $B = -13\gamma_c$ (dashed line) of the external magnetic field. Other employed parameters are $\Omega_c = 40\gamma$, $\Delta_c = 0$, $\Delta_p = 0$ (a) and $\Delta_p = 19\gamma$ (b).

parameters are $\Omega_c = 40\gamma$ and $\Delta_c = 0$. As indicated in figure 7, when the magnetic field is absent $B = 0$, Kerr nonlinear coefficient is zero at the two-photon resonance of probe and coupling fields $\Delta_p = \Delta_c = 0$ and is maximum at the frequency detuning $\Delta_p = 19\gamma$. Otherwise, when the magnetic field is present with $B = -13\gamma_c$, the nonlinear coefficient is maximum at $\Delta_p = 0$ and is zero at $\Delta_p = 19\gamma$. Therefore, from figure 10(a) we can see that at $\Delta_p = 0$ there is no OB behavior when $B = 0$ (see the solid line), however, the OB behavior has appeared when $B = -13\gamma_c$ (see the dashed line). Similarly, the OB behavior at $\Delta_p = 19\gamma$ when

$B = 0$ (see the solid line of figure 10(b)) is disappeared when $B = -13\gamma_c$.

Besides, the variations of the Kerr nonlinearity in figure 9 also lead to the change of the OB behaviors with respect to the intensity and frequency of the coupling field as demonstrated in figure 11. It shows that when increasing the Rabi frequency Ω_c from 25γ to 32γ or decreasing the frequency detuning Δ_c from 6γ to 0 , the magnitude of Kerr nonlinear coefficient is also increased. Therefore, the OB behavior appears more clearly; however, in these regions, the probe field absorption increases, so that the OB thresholds also increase.

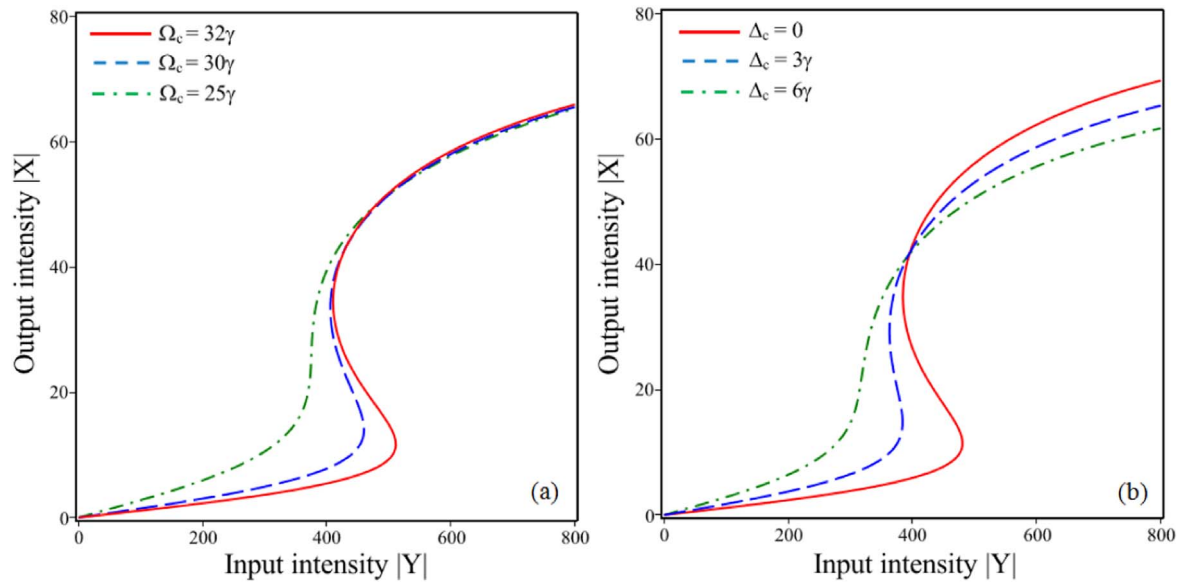


Figure 11. The input-output intensity curves at different values of the Rabi frequency when $\Delta_c = 0$ (a) and the frequency detuning when $\Delta_c = 40\gamma$ (b) of the coupling field. Other parameters are $\Delta_p = 0$ and $B = 13\gamma_c$.

4. Conclusion

We have studied the modification of absorption, dispersion, group index, Kerr nonlinearity, and optical bistability of degenerated three-level V-type EIT medium by the external magnetic field. By changing the strength or the sign of the magnetic field, electromagnetically induced transparency is converted to electromagnetically induced absorption, and hence the dispersion response is also switched between normal and anomalous regimes. These lead to light propagation is changed from subluminal to superluminal regimes and vice versa. That is, for the given parameters of the probe and coupling fields we can be found the optimum magnetic field to attain the maximum value of the group index. The external magnetic field is also used to transform the zero value of the Kerr nonlinear coefficient in the resonant region into the positive or negative peaks and vice versa. The magnitude and the sign of the Kerr nonlinearity are changed by tuning the magnetic field. As a result, the OB behaviors are made to appear or disappear when turn-on/off of the external magnetic field. Moreover, the threshold intensity and the width of optical bistability are also controlled by the magnetic field or the intensity and frequency of the coupling beam.

Acknowledgments

This work has been funded by Vietnam's Ministry of Education and Training under Grant No. B2020-TDV-03.

ORCID iDs

Nguyen Huy Bang  <https://orcid.org/0000-0003-4702-3157>

Le Van Doai  <https://orcid.org/0000-0002-1850-3437>

References

- [1] Boller K J, Imamoglu A and Harris S E 1991 Observation of electromagnetically induced transparency *Phys. Rev. Lett.* **66** 2593
- [2] Doai L V, Trong P V, Khoa D X and Bang N H 2014 Electromagnetically induced transparency in five-level cascade scheme of ^{85}Rb atoms: an analytical approach *Optik* **125** 3666–9
- [3] Mousavi S M, Safari L, Mahmoudi M and Sahrai M 2010 Effect of quantum interference on the optical properties of a three-level V-type atomic system beyond the two-photon resonance condition *J. Phys. B: At. Mol. Opt. Phys.* **43** 165501
- [4] Fleischhauer M, Imamoglu A and Marangos J P 2005 Electromagnetically induced transparency: optics in coherent media *Rev. Mod. Phys.* **77** 633–73
- [5] Li Y Q and Xiao M 1995 Electromagnetically induced transparency in a three-level Λ -type system in rubidium atoms *Phys. Rev. A* **51** 2703–6
- [6] Zhao J, Wang L, Xiao L, Zhao Y, Yin W and Jia S 2002 Experimental measurement of absorption and dispersion in V-type cesium atom *Opt. Commun.* **206** 341–5
- [7] Li Y Q and Xiao M 1995 Electromagnetically induced transparency in ladder-type inhomogeneously broadened media: theory and experiment *Phys. Rev. A* **51** 576–84
- [8] Braunstein D, Koganov G A and Shuker R 2011 Dressed-state analysis of lasing without population inversion in a three-level ladder system: the temporal regime *J. Phys. B: At. Mol. Opt. Phys.* **44** 235402
- [9] Yadav K and Wasan A 2017 Sub-luminal and super-luminal light propagation in inverted-Y system with wavelength mismatching effects *Phys. Lett. A* **381** 3246–53
- [10] Anh N T, Doai L V and Bang N H 2018 Manipulating multi-frequency light in a five-level cascade-type atomic medium associated with giant self-Kerr nonlinearity *J. Opt. Soc. Am. B* **35** 1233
- [11] Doai L V 2020 The effect of giant Kerr nonlinearity on group velocity in a six-level inverted-Y atomic system *Phys. Scr.* **95** 035104
- [12] Dutta S 2011 The incoherent pump rate: an optical tool for controlling the probe response and dispersion in a three-level

- Λ system in the presence of spontaneously generated coherence *Phys. Scr.* **83** 015401
- [13] Xiong W and Ye L 2011 Schemes for entanglement concentration of two unknown partially entangled states with cross-Kerr nonlinearity *J. Opt. Soc. Am. B* **28** 2030
- [14] Khoa D X, Doai L V, Son D H and Bang N H 2014 Enhancement of self-Kerr nonlinearity via electromagnetically induced transparency in a five-level cascade system: an analytical approach *J. Opt. Soc. Am. B* **31** 1330
- [15] Hamed H R and Juzeliunas G 2015 Phase-sensitive Kerr nonlinearity for closed-loop quantum systems *Phys. Rev. A* **91** 053823
- [16] Hamed H R, Gharamaleki A H and Sahrai M 2016 Colossal Kerr nonlinearity based on electromagnetically induced transparency in a five-level double-ladder atomic system *App. Opt.* **55** 5892–9
- [17] Xiong W, Jin D-Y, Qiu Y, Lam C-H and You J Q 2016 Cross-Kerr effect on an optomechanical system *Phys. Rev. A* **93** 023844
- [18] Bang N H, Khoa D X, Son D H and Doai L V 2019 Effect of Doppler broadening on giant self-Kerr nonlinearity in a five-level ladder-type system *J. Opt. Soc. Am. B* **36** 3151
- [19] Doai L V 2019 Giant cross-Kerr nonlinearity in a six-level inhomogeneously broadened atomic medium *J. Phys. B: At. Mol. Opt. Phys.* **52** 225501
- [20] Asadpour S H, Sahrai M, Soltani A and Hamed H R 2012 Enhanced Kerr nonlinearity via quantum interference from spontaneous emission *Phys. Lett. A* **376** 147–52
- [21] Gao H, Sun H, Fan S and Zhang H 2016 Phase control of Kerr nonlinearity in V-type system with spontaneously generated coherence *J. Mod. Opt.* **63** 598–604
- [22] Luo X-Q, Li Z-Z, Li T-F, Xiong W and You J Q 2018 Tunable self-focusing and self-defocusing effects in a triple quantum dot via the tunnel-enhanced cross-Kerr nonlinearity *Opt. Exp.* **26** 32585
- [23] Bang N H, Khoa D X, An N L T, Sau V N, Son D H and Doai L V 2019 Influence of Doppler broadening on cross-Kerr nonlinearity in a four-level inverted-Y system: an analytical approach *J. Non. Opt. Phys. Mat.* **28** 1950031
- [24] Sahrai M, Hamed H R and Memarzadeh M 2012 Kerr nonlinearity and optical multi-stability in a four-level Y-type atomic system *J. Mod. Opt.* **59** 980–7
- [25] Khoa D X, Doai L V, Anh L N M, Trung L C, Thuan P V, Dung N T and Bang N H 2016 Optical bistability in a five-level cascade EIT medium: an analytical approach *J. Opt. Soc. Am. B* **33** 735–40
- [26] Sahrai M, Asadpour S H, Mahrami H and Sadighi-Bonabi R 2011 Controlling the optical bistability via quantum interference in a four-level N-type atomic system *J. Lumin.* **131** 1682–6
- [27] Wang Z, Chen A X, Bai Y, Yang W X and Lee R K 2012 Coherent control of optical bistability in an open Λ -type three-level atomic system *J. Opt. Soc. Am. B* **29** 2891–6
- [28] Buica B and Nakajima T 2014 Propagation of two short laser pulse trains in a Λ -type three-level medium under conditions of electromagnetically induced transparency *Opt. Commun.* **332** 59
- [29] Dong H M, Doai L V and Bang N H 2018 Pulse propagation in an atomic medium under spontaneously generated coherence, incoherent pumping, and relative laser phase *Opt. Commun.* **426** 553
- [30] Qi Y, Niu Y, Zhou F, Peng Y and Gong S 2011 Phase control of coherent pulse propagation and switching based on electromagnetically induced transparency in a four-level atomic system *J. Phys. B: At. Mol. Opt. Phys.* **44** 085502
- [31] Anton M A, Carreno F, Calderon O G, Melle S and Gonzalo I 2008 Optical switching by controlling the double-dark resonances in a N-tripod five-level atom *Opt. Commun.* **281** 6040–8
- [32] Fountoulakis A, Terzis A F and Paspalakis E 2010 All-optical modulation based on electromagnetically induced transparency *Phys. Lett. A* **374** 3354
- [33] Bang N H, Khoa D X and Doai L V 2019 Controllable optical properties of multiple electromagnetically induced transparency in gaseous atomic media *Comm. Phys.* **28** 1–33
- [34] Cox K, Yudin V I, Taichenachev A V, Novikova I and Mikhailov E E 2011 Measurements of the magnetic field vector using multiple electromagnetically induced transparency resonances in Rb vapor *Phys. Rev. A* **83** 015801
- [35] Mitra S, Dey S, Hossain M M, Ghosh P N and Ray B 2013 Temperature and magnetic field effects on the coherent and saturating resonances in Λ - and V-type systems for the ^{85}Rb -D2 transition *J. Phys. B: At. Mol. Opt. Phys.* **46** 075002
- [36] Slavov D, Sargsyan A, Sarkisyan D, Mirzoyan R, Krasteva A, Wilson-Gordon A D and Cartaleva S 2014 Sub-natural width N-type resonance in cesium atomic vapour: splitting in magnetic fields *J. Phys. B: At. Mol. Opt. Phys.* **47** 035001
- [37] Kaur P and Wasan A 2017 Effect of magnetic field on the optical properties of an inhomogeneously broadened multilevel Λ -system in Rb vapor *Eur. Phys. J. D* **71** 78
- [38] Cheng H, Wang H M, Zhang S S, Xin P P, Luo J and Liu H P 2017 Electromagnetically induced transparency of ^{87}Rb in a buffer gas cell with magnetic field *J. Phys. B: At. Mol. Opt. Phys.* **50** 095401
- [39] Mishra C, Chakraborty A, Srivastava A, Tiwari S K, Ram S P, Tiwari V B and Mishr S R 2018 Electromagnetically induced transparency in Λ -systems of ^{87}Rb atom in magnetic field *J. Mod. Opt.* **65** 2269–77
- [40] Asadpour S H, Hamed H R and Soleimani H R 2015 Slow light propagation and bistable switching in a graphene under an external magnetic field *Laser Phys. Lett.* **12** 045202
- [41] Karimi R, Asadpour S H, Batebi S and Soleimani H 2015 Manipulation of pulse propagation in a four-level quantum system via an elliptically polarized light in the presence of external magnetic field *Mod. Phys. Lett. B* **29** 1550185
- [42] Bang N H, Khoa D X and Doai L V 2020 Controlling self-Kerr nonlinearity with an external magnetic field in a degenerate two-level inhomogeneously broadened medium *Phys. Lett. A* **384** 126234
- [43] Yu R, Li J, Ding C and Yang X 2011 Dual-channel all-optical switching with tunable frequency in a five-level double-ladder atomic system *Opt. Commun.* **284** 2930–6
- [44] Li J, Yu R, Si L and Yang X 2010 Propagation of twin light pulses under magneto-optical switching operations in a four-level inverted-Y atomic medium *J. Phys. B: At. Mol. Opt. Phys.* **43** 065502